encit 2020

ABCM Associação Brasileira de Engenharia e Ciências Mecânicas

18th Brazilian Congress of Thermal Sciences and Engineering
November 16–20, 2020 (Online)

ENC-2020-0413
PARAMETRIC OPTIMIZATION OF A SUPERSONIC SWIRLING SEPARATOR

Jairo P. Cavalcante
Arthur S. Cato
Luccas K. Kavabata
Ulisses A. S. Costa
Ernani V. Volpe, PhD, Assoc. Prof.
University of São Paulo; Av. Prof. Mello Moraes 2231, Office TS-13, São Paulo-SP; 05508-030, Brazil
jairo.pcfilho@gmail.com, arthur.cato@gmail.com, luccas.kavabata@usp.br, eng.ulissessilva@gmail.com, ernvolpe@usp.br

Marcelo T. Hayashi, PhD, Adj. Prof.
Federal University of ABC; Bloco Delta, Sala 384, CECS, São Bernardo do Campo-SP; 09606-045, Brazil
marcelo.hayashi@ufabc.edu.br

Abstract. *Supersonic separators of carbon dioxide (CO_2) consist in a relatively new technology which addresses two key factors in the Natural Gas processing: Firstly, it efficiently removes most of the carbon dioxide present in the natural gas composition, for high concentrations of carbon dioxide; and secondly, it can fit in the reduced space available on the Floating Production Storage and Offloading (FPSOs) units. Using adjoint method, two measure of merit are proposed to enhance the separator geometry: (1) pressure inverse design to delay the shock wave in the nozzle; and (2) the angular moment, to increase the swirl number, by slightly modificating the swirler vanes geometry. Both objectives have been succesfully achieved, keeping most of the separator original footprint and also confirmed the right choice in the measures of merit.*

Keywords: *swirling, adjoint, supersonic, optimization, method*

1. INTRODUCTION

The technology of the supersonic separation appeared about 50 years ago, and since then it is being progressively developed. In 1968, Garret (Haghighi *et al.*, 2015; Goo, 2016) proposed a device for the separation of heavy gaseous components in a mixture through a convergent-divergent nozzle linked to a curved channel (which executes the same function as a swirling flow, by separating the condensed substances through inertial action). The device of Garret inspired other techniques, such as *Linhardt and Beveridge*, 1981 (Haghighi *et al.*, 2015), whose approach is very similar to the first one, and the *Nasikas*, 1994 (Haghighi *et al.*, 2015), which again uses a swirling flow for the multiphase separation of gases, but introduces normal shock waves to decelerate the central flow, and to end the separation of the components. Currently, the main suppliers of the technology that uses swirling flows are the companies Engo 3S and Twister BV (Eng, 2016; Twi, 2016). Both companies started around the year 2000. The primordial difference between Engo 3S and TwisterBV approaches lies in the way to obtain the swirling: The (Eng, 2016) model employs fixed vanes connected to the inner walls of the separator, while the (Twi, 2016) presents a central body with fixed vanes. The vanes are responsible for the swirling. The Engo 3S model uses a more conventional De Laval nozzle geometry. The main representative of the technology which uses a curved channel (similar to the one proposed by Garret) is Orbital Alliant TechSystems (OrbitalATK), whose first proof of concept design dates back to 2010. According to Orbital, the cost per ton of CO_2 avoided is about half the one incurred by using amine based extraction (Orb, 2015). Additional details on the current players in supersonic separation can be found in (Cavalcante Filho, 2020).

2. SCOPE AND OBJECTIVES

The project considers a supersonic separator as an assembly with two main components: The first one is the convergent-divergent nozzle, where the phase change processes take place and the second one is a stationary swirl generator, located before the convergent nozzle portion, which is responsible for the introduction of a rotation in the flow, thus allowing the centrifugal force to bounce droplets of liquid carbon dioxide to the internal wall of the divergent nozzle region.

In this work, the swirler has been created with seven fixed vanes of complex shape, with expressive camber, not

following any kind of known airfoil geometry. The nozzle has been defined using the geometry proposed by Renzo Arina (Arina, 2004), usually known as the Arina profile, since it appears in a number of articles in the literature. The Arina nozzle profile expression is:

$$A(x) = \begin{cases} 2.5 + 3(\frac{x}{x_{th}} - 1.5)(\frac{x}{x_{th}})^2; & \forall x \leqslant x_{th} \\ 3.5 - \frac{x}{x_{th}}[6 - 4.5\frac{x}{x_{th}} + (\frac{x}{x_{th}})^2] & \forall x \geqslant x_{th} \end{cases} \tag{1}$$

Figure 1, shows the 3D supersonic separator schematic view, which has been employed in the project.

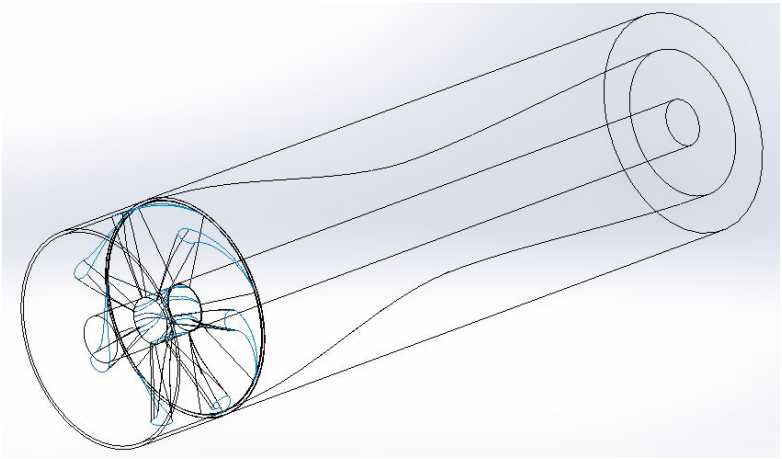

Figure 1. Supersonic Swirling Separator schematic aspect.

The optimization problem has been tackled in two phases: In the first phase, the nozzle portion has been treated as a 2D entity with symmetry, using Euler equations: the preliminary simulations have considered the CST parametrization, which has been implemented in the CFD tool (SU2) and superseded the use of the standard Hicks-Henne bump functions, owing to the better CST results, that is, it has been possible to delay the shock waves somewhat nearer to the outlet than using Hicks-Henne functions. The swirler device has been tackled in the second phase, using 3D Navier-Stokes with FFD parametrization (Bézier) parametrization. The turbulence model has been the SST one (Menter's Shear Stress Transport, (Menter, 1994, 2009; Smirnov and Menter, 2009; Alahmadi and Nowakowski, 2016)).

3. METHODOLOGY

For all project phases, the adopted method to evaluate the geometric sensitivities has been the *Adjoint Method* and the optimization used has been the *Steepest Descent* method. The CFD tool that has been chosen to carry out this project is the open source code SU^2 or $SU2$, (Palacios and Economon, 2013, 2014). It is a flow solver and an adjoint solver, with several standard measures of merit available. A diagram of the process of optimization using the adjoint method is shown in Fig. 2. Essentially, the adjoint method is a powerful tool to compute the sensitivity (that is, the gradient) of a given measure of merit, with respect to parameters that control the boundary conditions of a physical system. That system is assumed to be governed by a set of Partial Differential Equations (PDEs), and the measure of merit is taken to be a functional (an objective functional, as it is also called). In this work, the flow represents the physical system and the objective functionals usually depend on flow variables and on the shape and location of the boundaries (Jameson *et al.*, 1998, 2003). The adjoint method has proven to be a powerful tool for optimizing complex systems, where a high fidelity representation of the physics is essential (Zingg *et al.*, 2008).

The adjoint method has shown to be particularly suitable to tackle problems with large number of control parameters and few measures of merit (that is, few objective functions), and several possibilities of optimum criteria. For it only requires two converged solutions to compute sensitivity gradients, regardless of their dimensionality and for any particular measure of merit. This translates in lower computational cost, when compared with other methods such as finite differences or genetic algorithms (Ceze, 2008). In the nozzle optimization work of this project, the definition of objective function for inverse design applications (I) is given by the mean square error of the actual pressure distribution p with respect to a target pressure distribution p_{tar}, on the separator internal wall:

$$I = \frac{1}{2} \int_{b_w} (p - p_{tar})^2 \, \mathrm{d}s \tag{2}$$

The target pressure distribution p_{tar} is what one imposes to modify a surface (b_w) where the pressures are evaluated, without knowing whether it will be possible or not. Equation (2) can be rewritten, in terms of *pressure coefficient*, as

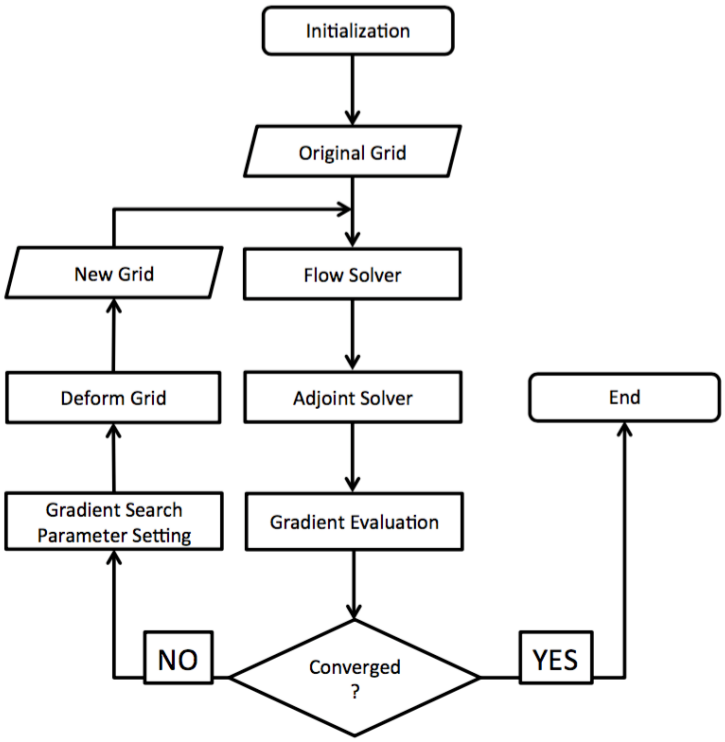

Figure 2. Optimization loop diagram using the *Adjoint Method*.

$$I = \frac{1}{2} \int_{b_w} (C_p - C_{p_{tar}})^2 \, \mathrm{d}s \tag{3}$$

where C_p represents the *pressure coefficient*.

In the optimization of the vanes geometry, the radial (angular) moment in the axial direction has been used as the measure of merit. The two measures of merit used in the project are included among the standard ones available in the SU2 libraries. Owing to those characteristics, the adjoint method has been the subject of intense research activity. It has spawned a wide variety of applications, ranging from nuclear reactor thermo–hydraulics (Cacuci *et al.*, 1980) to aerodynamics (Jameson *et al.*, 1997) and the design of ship hulls (Jameson and Martinelli, 2007): It is the versatility and the high fidelity representation of the physics, the main motivation to employ the adjoint method in this work.

3.1 Adjoint Method Overview

The material on this introduction regarding adjoint method expanded far beyond the common geometric sensitivities, follows very closely the work (Hayashi *et al.*, 2017), which was a natural extension of (Hayashi *et al.*, 2013). As was mentioned earlier, the optimization of the supersonic separator that is undertaken here is mostly a geometric optimization. However, there is a possibility of exploring inflow and outflow conditions, or at least, to point directions to explore them in subsequent projects.

The adjoint method has been established as a major contribution in the aerodynamics field, thanks to the works of pioneers like Lions (1971), Pironneau (1973, 1974, 1983); Mohamadi and Pironneau (2000), Jameson (1988, 1995), Giles and Pierce (1998, 2000), Cacuci *et al.* (1980) and others.

Over the years since its extension to transonic flows by Jameson in a landmark work (Jameson, 1988), the adjoint method has become a veritable field of research in the aerodynamics and CFD communities. It has been the subject of extensive investigation and spawned a large variety of applications, ranging from design optimization to flow stability analysis, error estimation and mesh adaptation, and uncertainty quantification.

As a first reference (Cacuci *et al.*, 1980), Cacuci *et alii* have formally established the theoretical basis behind the adjoint method of sensitivity analysis for nonlinear systems. Two equally relevant works by the same author followed soon after, with an in–depth analysis of the mathematical foundations underlying the method. The first one (Cacuci, 1981a) discusses the necessary and sufficient conditions for the existence and uniqueness of adjoint operators, whereas the second (Cacuci, 1981b) extends the scope of the adjoint formalism to a larger variety of responses, which includes general operators. It is worth adding that, along with his collaborators, that author went on to publish a number of relevant references on a wide

range of applications of the method (Cacuci and Wacholder, 1982; Cacuci, 1990; Cacuci and Ionescu-Bujor, 1990, 2005; Ionescu-Bujor *et al.*, 2005; Cacuci, 2003; Cacuci *et al.*, 2005; Cacuci, 2015, 2016).

Two of the above works by Cacuci are especially relevant. In (Cacuci *et al.*, 1980), the author devises a sequence of formal steps to construct the adjoint problem. Whereas, in (Cacuci, 1981a), conditions for the existence and uniqueness of the adjoint operator require the underlying spaces to be complete and normed (*Banach*). They also demand that all operators that act upon the state vector admit densely defined partial Gâteaux derivatives with respect to all of their components (Luenberger, 1969; Lusternick and Sobolev, 1961), and that the Gâteaux differentials be linear in the state vector variations. The need for an inner product is met by further setting the problem in Hilbert spaces (Haaser and Sullivan, 1991), which are self–dual and where Riesz representation theorem ensures the operators uniqueness (Luenberger, 1969; Kreyszig, 1989; Dacorogna, 2004; Brezis, 2010). Next we present a brief account of those works, as they apply to the particular problem in hand. So as to put more emphasis on the formal, mathematical, aspects of proposed approach.

It starts by considering a measure of merit, an objective functional relative to Euler compressible flows. In generic form, it may be written as (Cacuci *et al.*, 1980):

$$I_o[\mathbf{Q},\alpha] = \int_{\mathcal{D}} \mathcal{F}[\mathbf{Q}(\chi),\alpha(\chi),\chi]\mathrm{d}\chi \tag{4}$$

where $\mathbf{Q}$ is the state vector, comprising density, linear momentum and total energy. While χ are coordinates of the domain $\mathcal{D}$ in physical space, $\mathcal{D} \subset \mathbb{R}^J$, and α represents the set of parameters that control the system, $\alpha \in \mathbb{R}^N$. In generic form, one has:

$$\mathbf{Q}(\chi) = [Q_1(\chi), \dots Q_K(\chi)] \quad ; \quad \chi = \left(\chi^1, \dots, \chi^J\right) \quad ; \quad \alpha(\chi) = [\alpha_1(\chi), \dots, \alpha_N(\chi)] \tag{5}$$

The state space is taken to be a K–dimensional Hilbert space ($\mathbf{Q} \in H_Q$) over the scalar field of real numbers $\mathbb{R}$. Inner products are defined on the basis of domain and surface integrals, respectively:

$$\langle \mathbf{f}, \mathbf{g} \rangle \equiv \int_{\mathcal{D}} \mathbf{f}(\chi) \cdot \mathbf{g}(\chi)\ \mathrm{d}\mathcal{V}_\chi \quad ; \quad \langle \mathbf{f}, \mathbf{g} \rangle_s \equiv \int_{\partial\mathcal{D}} \mathbf{f}(\chi) \cdot \mathbf{g}(\chi)\ \mathrm{d}S_\chi \tag{6}$$

and a L^2 norm is induced by that product: $\|\mathbf{f}\|^2 = \langle \mathbf{f}, \mathbf{f} \rangle$.

Given the well–known properties of Hilbert spaces, and the fact that Gâteaux differentials of the Euler equations and boundary conditions are linear on $\delta\mathbf{Q}$ and $\delta\alpha$, a unique set of adjoint Euler equations can be promptly derived (Volpe, 2016), which fully agrees with the literature on the method.

Under the above conditions, the objective functional I_o, eq. (4), is an application of type $H_Q \times \mathbb{R}^N \to \mathbb{R}$, which is defined in the flow domain $\mathcal{D} \subset \mathbb{R}^J$. A Vainberg theorem (number *3.2* in (Vainberg, 1964)) gives the necessary and sufficient conditions for a generic functional to have Gâteaux differential that are linear on the variations (Luenberger, 1969; Lusternick and Sobolev, 1961), what is used by Cacuci in establishing the theoretical foundation (Cacuci, 1981a,b). However, here we shall, *a priori*, confine the scope of the investigation to objective functionals that meet those conditions, that is, those with first variation of the form:

$$\delta I_o = \underbrace{\langle \mathcal{F}'_Q, \delta\mathbf{Q} \rangle}_{\delta I_{o_Q}} + \underbrace{\langle \mathcal{F}'_\alpha, \delta\alpha \rangle}_{\delta I_{o_\alpha}} \tag{7}$$

where δI_{o_Q} is the physical part and δI_{o_α} is the parametric part of the total variation. Again, in generic form, the physical system is governed by a set $\mathbf{N}$ of K nonlinear PDEs, which, in turn, are subject to a set $\mathbf{B}$ of boundary and initial conditions. In terms of operators, one can write Cacuci *et al.* (1980),

$$\mathbf{N}[\mathbf{Q}(\chi),\alpha] = \mathbf{R}(\chi,\alpha) \tag{8}$$

$$\mathbf{B}[\mathbf{Q}(\chi),\alpha]_s = 0 \tag{9}$$

where the subscript $[\ ]_s$ implies that the conditions are imposed on the appropriate domain boundaries $\partial\mathcal{D}$ and $\mathbf{R}(\chi,\alpha)$ is the source term of the equations which govern the flow. Then, in principle, one can define an augmented functional that represents the constrained variational problem,

$$G(\mathbf{Q},\alpha,\phi,\beta,\mathbf{a}) = I_o[\mathbf{Q},\alpha] - \langle \phi, \mathbf{N} - \mathbf{R} \rangle - \langle \beta, \mathbf{B} \rangle_s - \langle \mathbf{a}, \alpha - \alpha_o \rangle \tag{10}$$

Usually non–holonomic (Gelfand and Fomin, 1963; Liberzon, 2012; Goldstein *et al.*, 2000; Monforte, 2002), the constraints are introduced by the Lagrange multipliers ϕ, β and $\mathbf{a}$, in the last three functionals. The first, ϕ, imposes the governing equations and the second, β, enforces their boundary conditions. While the third, $\mathbf{a}$, ensures that the control parameters take on a given set of prescribed values $\alpha = \alpha_o$, which corresponds to the baseline configuration.

Naturally, the variation of G in eq. (10) depends on that of the governing equations (8) and boundary conditions (9). These have Gâteaux differentials that are given by:

$$\mathbf{L}\delta\mathbf{Q} = \mathbf{S}\delta\alpha \tag{11}$$

$$\mathbf{B}'_Q\delta\mathbf{Q} = -\mathbf{B}'_\alpha\delta\alpha \tag{12}$$

where the operators are defined as $\mathbf{L} \equiv \mathbf{N}'_Q$ and $\mathbf{S} \equiv \mathbf{R}'_\alpha - \mathbf{N}'_\alpha$, respectively Cacuci *et al.* (1980). The first, $\mathbf{L}$, is the linearized form of the governing equations, whereas the second, $\mathbf{S}$, gathers all parameter variations.

The first term on the right hand side of (10) is the measure of merit, for which the variation is given by (7). As for the second term, one must compute its Gâteaux derivative and substitute (11) for the corresponding terms. Then, on making use of Gauss' theorem, one can transfer the differential operators from the state vector $\mathbf{Q}$ to the Lagrange multiplier ϕ. That leads to:

$$-\langle\phi, \mathbf{L}\delta\mathbf{Q}\rangle = \langle\mathbf{L}^*\phi, \delta\mathbf{Q}\rangle - P[\phi, \delta\mathbf{Q}]_s \tag{13}$$

where the term $P[\phi, \delta\mathbf{Q}]_s$ is the bilinear concomitant the operation ensues (Cacuci *et al.*, 1980; Morse and Feshbach, 1953; Ince, 1956) and, again, the symbol $[\ ]_s$ refers to the domain boundaries $\partial\mathcal{D}$. Furthermore, the first term on the right hand side of (13) contains $\mathbf{L}^*$, which is the adjoint operator to $\mathbf{L}$.

Finally, by computing the Gâteaux diferentials of the remaining functionals and on combining them with the above results, one obtains the first variation of the augmented functional, δG. It reads,

$$\begin{aligned}\delta G = & -\langle\delta\phi, \mathbf{N} - \mathbf{R}\rangle - \langle\delta\beta, \mathbf{B}\rangle_s - \langle\delta\mathbf{a}, \alpha - \alpha_o\rangle + \left\langle\mathbf{L}^*\phi + \mathcal{F}'_Q, \delta\mathbf{Q}\right\rangle + \\ & - \left\langle\beta, \mathbf{B}'_Q\delta\mathbf{Q}\right\rangle_s - \left[\left\langle P_1(\phi), \mathbf{B}'_Q\delta\mathbf{Q}\right\rangle_s + \langle\mathbf{B}^*(\phi), \mathbf{M}\delta\mathbf{Q}\rangle_s\right] + \langle\mathcal{F}'_\alpha, \delta\alpha\rangle + \\ & + \langle\phi, \mathbf{S}\delta\alpha\rangle - \langle\mathbf{a}, \delta\alpha\rangle - \langle\beta, \mathbf{B}'_\alpha\delta\alpha\rangle_s\end{aligned} \tag{14}$$

where δI_o has already been replaced by eq. (7). In addition to that, the bilinear concomitant $P[\phi, \delta\mathbf{Q}]_s$ from (13) has been decomposed into the two terms within square brackets. Both of them are inner products, only they must be computed over the appropriate boundaries. The first one involves a $P_1(\phi)$ and the linearized boundary operator $\mathbf{B}'_Q\delta\mathbf{Q}$. While the second involves a $\mathbf{B}^*(\phi)$, which represents the adjoint boundary operator, and a term $\mathbf{M}\delta\mathbf{Q}$.

The decomposition of P is **not** unique, and neither are the definitions of P_1 and $\mathbf{M}$ (Cacuci *et al.*, 1980). On the contrary, the only restriction that is actually imposed on the procedure is that the operator $\mathbf{M}$ be linearly independent of $\mathbf{B}'_Q$. As a result of this, the very determination of the adjoint boundary problem hinges upon a non–unique decomposition, and it only makes sense that it should be this way. After all, there must be some leeway left to ensure the problem is well–posed.

The augmented functional G realizes extrema upon the condition that (14) vanishes for arbitrary, albeit realizable, variations of its parameters:

$$\delta G = 0 \ \ \forall \ \ \{\delta\mathbf{Q}, \delta\alpha, \delta\phi, \delta\beta, \delta\mathbf{a}\} \ \ \in \ \ \{\text{locus of realizability}\} \tag{15}$$

That, in turn, requires that the following conditions be met:

1. The equations that govern the physics (8) and their boundary conditions (9) are satisfied. In addition, the control parameters take on the prescribed baseline values, $\alpha = \alpha_o$. These requirements imply that the first three terms of (14) are identically zero.

2. On imposing the condition,

$$\beta = -P_1(\phi) \ \ , \tag{16}$$

one drives to zero the sum of the fifth and sixth terms of (14). This particular equation also solves the β in terms of the ϕ.

3. The vector ϕ must satisfy the adjoint equation, which is given by:

$$\mathbf{L}^*\phi + \mathcal{F}'_Q = 0 \ \ , \tag{17}$$

as it appears in the fourth term of (14). The corresponding boundary conditions are given by the operator

$$\mathbf{B}^*(\phi) = 0 \ \ , \tag{18}$$

which comes from the seventh term in that equation. Equation (18) determines ϕ at the boundaries, along with the β thereof.

4. The vector $\mathbf{a}$ is specified by the following condition:

$$\langle \mathbf{a}, \delta\alpha \rangle = \langle \mathcal{F}'_\alpha, \delta\alpha \rangle + \langle \phi, \mathbf{S}\delta\alpha \rangle - \langle \beta, \mathbf{B}'_\alpha \delta\alpha \rangle_s \tag{19}$$

which collects all the remaining terms when $\delta G = 0$. In fact, this is the realizable part of the sensitivity gradient, δI_o, as will be shown next.

To prove the above statement regarding the sensitivity gradient (Cacuci *et al.*, 1980), suffices it to recognize that: If the governing equations, (8) and (9) are identically satisfied for a given variation ΔG, of any size. Then, from the very definition of G in (10), it comes that

$$\begin{aligned} &\Delta G = \Delta I_o - \langle \mathbf{a}, \Delta\alpha \rangle \\ &\text{for} \begin{cases} \Delta G = G(\mathbf{Q}_2, \alpha_2; \phi_2, \beta_2, \mathbf{a}_2) - G(\mathbf{Q}_1, \alpha_1; \phi_1, \beta_1, \mathbf{a}_1) \\ \Delta I_o = I_o(\mathbf{Q}_2, \alpha_2) - I_o(\mathbf{Q}_1, \alpha_1) \\ \Delta\alpha = \alpha_2 - \alpha_1 \end{cases} \end{aligned} \tag{20}$$

In particular for an infinitesimal variation $\Delta G \to \delta G$, under the above conditions and where ϕ, α and β fulfill the above four requirements, there must correspond a stationary value of G. Therefore, one can write

$$\begin{aligned} \delta G &= \delta I_o - \langle \mathbf{a}, \delta\alpha \rangle = 0 \\ \delta I_o &= \langle \mathbf{a}, \delta\alpha \rangle \\ \delta I_o &= \langle \mathcal{F}'_\alpha, \delta\alpha \rangle + \langle \phi, (\mathbf{R}'_\alpha - \mathbf{N}'_\alpha)\, \delta\alpha \rangle + \langle P_1(\phi), \mathbf{B}'_\alpha \delta\alpha \rangle_s \end{aligned} \tag{21}$$

where the eqs. (16), (19) and the definition of $\mathbf{S}$ have been used. With the above expression (21), one can estimate the sensitivity gradient on the basis of the adjoint solution ϕ and parameter variations $\delta\alpha$, alone.

It is worth noting here that all physical variations $\delta\mathbf{Q}$ have been successfully removed from the gradient expression. Moreover, the first term on the right hand side of (21) is precisely δI_{o_α}, whereas the second measures the direct effects of $\delta\alpha$ on the governing equations, and the third does so with respect to their boundary conditions.

4. SEPARATOR GEOMETRY OPTIMIZATION

As earlier said, the separator optimization has been divided into two phases. In the first phase, only the nozzle has been optimized using 2D Euler equations. In the second phase, the complete separator assembly (nozzle and swirler) has been tackled with the 3D Navier-Stokes equations.

4.1 Nozzle Optimization

The flow simulation was solved with Euler 2D formulation, using methane as an ideal gas (this way, the stagnation pressure, the stagnation temperature, the stagnation enthalpy and the entropy are easily obtained). The optimization via inverse design simulation used C_p (pressure coefficient on the wall) directive, Eq. (3). The three parameters defined for the inlet were: Inflow temperature, 288.0 K, inflow static pressure, 100000 Pa and flow direction according to the x cartesian direction. In the outlet, the only parameter set up was the static back pressure, 83049.0 Pa. These parameters are the ones used in the article of Renzo Arina (Arina, 2004). The flow solver calculates the boundary conditions based on the parameters informed (temperature, static pressures, flow direction): in the inlet section, the boundary conditions are stagnation pressure and stagnation temperature; and in the outlet section, the boundary condition being the static back pressure itself. In all figures, where the nozzle profile is shown, the botton straight line represents its center line, and the top curve is the nozzle wall (either the original Arina profile, described in equation (1); or the optimized profile, obtained through the inverse design). The Arina meshes have been adjusted to allow good computational performance while keeping the desired accuracy: thus the "optimum" mesh which has been largely employed in most of the simulatios is a grid with 85504 triangles. Geometry deformation is based on CST (Kulfan and Bussoletti, 2006) parametrization with the number of design variables being 15. The convergence criterion is based on residual and the maximum residual is set up to 10^{-8}. The fluid used in the Arina nozzle optimization is methane, considered as an ideal gas, where the state of stagnation is reached through a reversible and adiabatic process (Hodge and Koenig, 2016) which allows one to check the sanity of solution by easily calculating the stagnation properties. The target $C_{p_{tar}}$ distribution is proposed on the basis of the designer knowledge and it is not necessarily realizable (Ceze, 2008).

The final optimization cycle has been the 17th one: Figure 3 compares respectively, the *pressure coefficient* (Cp), the *mach number* and the *geometry* with the target values. The values shown, are those obtained in the 17th optimization cycle with the same conditions of inlet and outlet as in the original Arina profile. In each graph, red curves or points represent the original flow solver outputs for the original Arina profile, blue curves or points represent the values resulting in the 17th optimization cycle and magenta curves or points represent the target values.

In this phase, the formation of a shock wave has been successfully delayed. Also, as a consequence of such delay, the temperature just upstream from the shock has gotten even lower. The shock in the optimized geometry became also

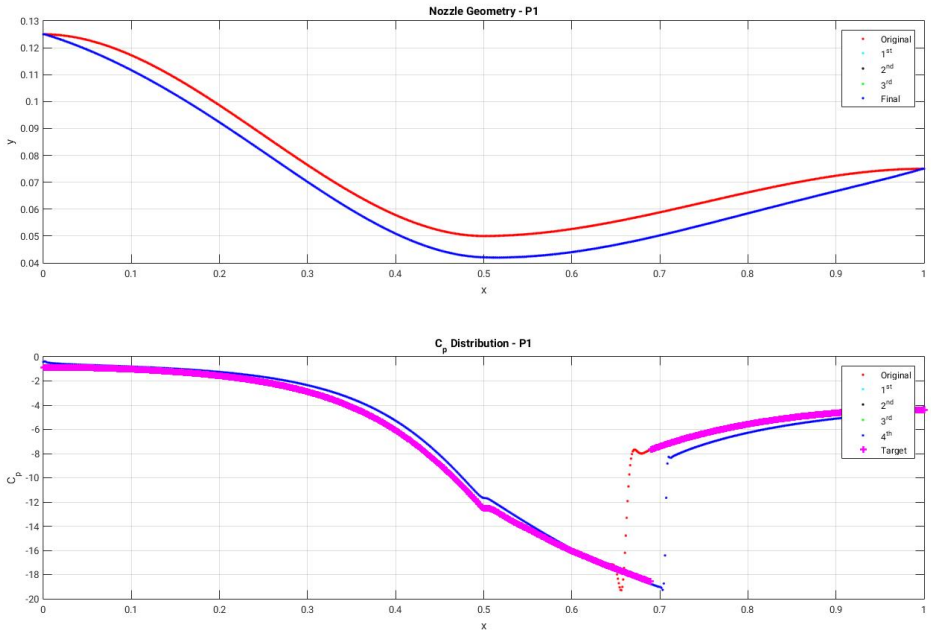

Figure 3. Original Geometry versus Optimized Geometry: red corresponds to the original Arina profile values and blue corresponds to the 17th optimization cycle values in conjunction with the corresponding data regarding the Pressure Coefficient for methane as a perfect gas. Intermediate initial cycles ($1^{st}...4^{th}$) have been removed to better reading.

stronger. The footprint of the nozzle has been kept, with a smaller throat diameter. The objective to slightly change the geometry has been reached in a realizable flow solution:

4.2 Complete Separator Optimization

The swirler is the part of the separator which precedes the nozzle. Its mission is to generate the cyclonic flow, which produces a high radial acceleration, thus bouncing the denser (liquid) particles to the separator internal walls, allowing the capture of the liquid carbon dioxide. It is formed by seven twisted vanes equally spaced: even thought this number could have been determined by using genetic optimization, in this case, its has been simply chosen as a mean to get expressive camber in the vanes profile. The vane angle of attack is zero and its profile does not follow any cataloged geometry: it has been created by the author. The purpose in this phase, is to increase the radial moment in the axial direction (which coincides with the hub center). This new function is named the "MOMENT–X" in the SU2 code: it is part of the code standard library of objective functions. Using the notation of (Beér and Chigier, 1972), the non-dimensional number which defines the swirl intensity, the swirl number, S, for a swirler which has a hub, is:

$$S = \frac{G_\varphi}{R_{so} G_x} \tag{22}$$

where

$$G_\varphi^a = \int_{R_{si}}^{R_{so}} (Wr) \rho U 2\pi r \mathrm{d}r \tag{23}$$

and

$$G_x^a = \int_{R_{si}}^{R_{so}} (U) \rho U 2\pi r \mathrm{d}r \tag{24}$$

R_{so} and R_{si} are, respectively, the outer and the inner radii of the swirler annulus, and the variables in the integrands of (23) and (24), are:

W = Tangential velocity component
U = Axial velocity component
r = Radius
ρ = Fluid density

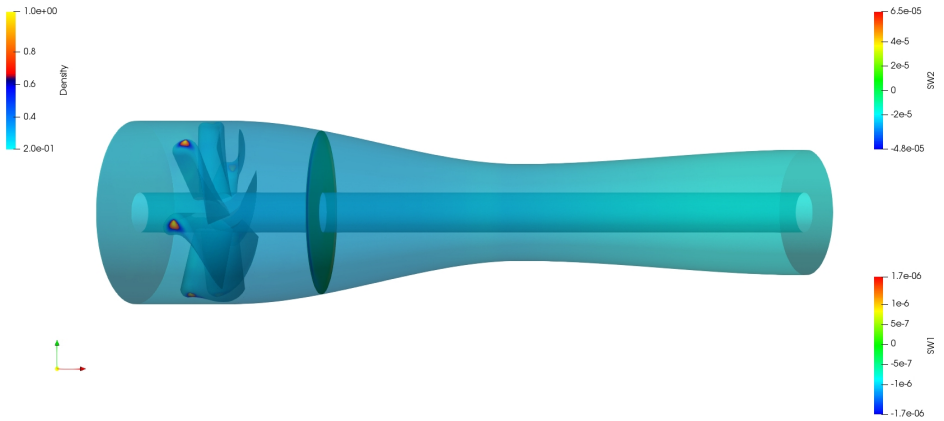

Figure 4. Transparent view of the Supersonic Swirling Separator, which scales for density, axial flux of the tangential momentum ($SW1$) and axial flux of the axial momentum ($SW2$). The momenta are integrated on the disc region to allow the calculation of the Swirl number. Output according to the 3D Navier-Stokes. Although three scales are shown (one for $density$, other for $SW1$ and another for $SW2$, only the $density$ scale is active).

Figure 4 shows the interior of the separator and the position where the strong Swirl number is found: The Swirl number is computaded for the disc region, with $R_{so} = 0.0685$. The used formulation is 3D Navier-Stokes, with no slip, an initial grid of 12465980 tetrahedral elements, using two-equations Menter's Shear Stress Transport (SST), which is described in (Menter, 1994).

The MOMENT–X, the torque that acts upon the swirler is very important, since it corresponds to the amount of swirl that the device imparts to the flow is profoundly tied to the swirling flow, since the larger the swirl intensity, the larger the moment in the axial direction is: The goal has been to improve the vanes geometry in order to enhance the MOMENT–X as a whole (that is, including the effect of all of the seven vanes). Owing to axial symmetry, the resulting moment should be aligned with the device axis, thus lacking components along the y and z directions.

Table 1 shows the Swirl number per cycle ($S = G_\varphi/(R_{so}G_x)$), of selected samples of a typical optimization job, using MOMENT–X as the measure of merit: Cycle 1 represents the original geometry. The table also shows the current values of the outer annulus radius, R_{so}; the axial flux of the tangential (or angular) momentum, G_φ; and the axial flux of the axial momentum (or thrust), G_x.

Table 1. Swirl numbers per optimization cycle, calculated for abscissa $x = 0.155$. Cycle 1 represents the original geometry. Cycle 32 is the last realizable cycle.

Swirl number per cycle				
$Cycle$	$Swirl\ number\ (S)$	R_{so}	G_φ	G_x
1	0.397694	0.129157	2.743998E-11	5.342155E-10
31	1.080520	0.129157	1.338033E-10	9.587732E-10
32	2.998887	0.129158	1.575179E-10	4.066760E-10

4.3 Final Considerations

In this work, a Supersonic Swirling Separator has been analyzed and optimized using the open source code SU2. The activities have included 2D and 3D simulations using, respectively, Euler and Navier-Stokes equations. The initial nozzle profile has been based on the Arina's nozzle and the swirler vanes have been created with no constraints in complexity. Two of the *measures of merit* available in the SU2 standard libraries, have been evaluated, the Inverse Design Pressure (INVERSE–DESIGN–PRESSURE) and the angular moment in the axial direction (MOMENT–X). Inverse design pressure has been successfully employed during the 2D nozzle optimization to delay the shock wave (together CST parametrization), and MOMENT–X has been confirmed as a good choice to increase the Swirl number (during the 3D simulations with Navier-Stokes equations): in increasing that moment, a corresponding increased boost in the swirl intensity is obtained. This matches two purposes: Firstly, it provides more room and lower temperatures to the change phase

processes, thus enhancing the separator performance and keeping the shape deformation to a minimum, which brings as a bonus, that the separator's footprint is also preserved at the same time. Secondly, the increase in the swirl intensity, also implies in a increased amount of droplets of condensed material which are radially bounced to the separator walls, facilitating their collection. The results have met the expectations based on theoretical grounds. The complete 3D separator optimization has run on high performance computation (HPC) facilities.

5. ACKNOWLEDGEMENTS

Jairo P. Cavalcante Filho wants to thank to STI-USP (Superintendência de Tecnologia da Informação da Universidade de São Paulo) for the HPC environment and support; and to FUSP (Fundação de Apoio à Universidade de São Paulo) for the funding throughout this project.

6. REFERENCES

, 2015. "Orbitalatk". `www.orbitalatk.com`. Accessed: 27/03/2018.

, 2016. "Engo3s". `http://www.engo3s.com/3s-technology`. Accessed: 05/07/2017.

, 2016. "Google-patents". `https://www.google.ch/patents/US3528216`. Accessed: 05/01/2017.

, 2016. "Twisterbv". `www.twisterbv.com`. Accessed: 05/08/2017.

Alahmadi, Y.H. and Nowakowski, A.F., 2016. "Modified shear stress transport model with curvature correction for the prediction of swirling flow in a cyclone separator". *Chemical Engineering Science*, Vol. 147, pp. 150–165.

Arina, R., 2004. "Numerical simulation of near critical fluids". *Applied Numerical Mathematics*, Vol. 51, pp. 409–426.

Beér, J.M. and Chigier, N.A., 1972. *Combustion Aerodynamics*. Halsted – John Wiley and Sons, INC, New York.

Brezis, H., 2010. *Functional Analysis, Sobolev Spaces and Partial Differencial Equations*. Springer, New York.

Cacuci, D.G., 1981a. "Sensitivity theory for nonlinear systems: I. nonlinear functional analysis approach". *J. Math. Phys., Vol. 22 p. 2794 to 2802*.

Cacuci, D.G., 1981b. "Sensitivity theory for nonlinear systems: Ii. extensions to additional classes of responses". *J. Math. Phys., Vol. 22 p. 2803 to 2812*.

Cacuci, D.G., 1990. "Global optimization and sensitivity analysis". *Nuclear Science and Engineering V. 104 p. 78 to 88*.

Cacuci, D.G., 2003. *Sensistivity and Uncertainty Analysis: Theory, Vol. 1*. Chapman & Hall/CRC, Boca Raton.

Cacuci, D.G., 2015. "Second–order adjoint sensitivity analysis methodology (2nd–asam) for computing exactly and efficiently first and second–order sensitivities in large–scale linear systems: I. computational methodology". *Journal of Computational Physics, Vol. 284 p. 687 to 699*.

Cacuci, D.G., 2016. "Second–order adjoint sensitivity analysis methodology (2nd–asam) for large–scale nonlinear systems: I. theory". *Nuclear Science and Engineering, Vol. 184 p. 16 to 30*.

Cacuci, D.G. and Ionescu-Bujor, M., 1990. "Global optimization and sensitivity analysis". *Nuclear Science and Engineering V. 136 p. 59 to 84*.

Cacuci, D.G. and Ionescu-Bujor, M., 2005. "Deterministic local sensitivity analysis of augmented systems: I. theory". *Nuclear Science and Engineering V. 151 p. 55 to 66*.

Cacuci, D.G., Ionescu-Bujor, M. and Navon, M.I., 2005. *Sensistivity and Uncertainty Analysis: Sensitivity and Uncertainty Analysis: Applications to Large Scale Systems Theory, Vol. 2*. Chapman & Hall/CRC, Boca Raton.

Cacuci, D.G. and Wacholder, E., 1982. "Adjoint sensitivity analysis for transient two–phase flow". *Nuclear Science and Engineering V. 104 p. 461 to 468*.

Cacuci, D.G., Weber, F., C., M., O.E. and Marable, J.H., 1980. "Sensitivity theory for general systems of non–linear equations". *Nuclear Science and Engineering*, Vol. 75, pp. 88–110.

Cavalcante Filho, J.P., 2020. *Parametric Optimization of a Supersonic Swirling Separator*. Master's thesis, University of São Paulo.

Ceze, M.A.B., 2008. *Projeto Inverso Aerodinâmico Utilizando o Método Adjunto Aplicado às Equações de Euler*. Master's thesis, University of São Paulo.

Dacorogna, B., 2004. *Introduction to the Calculus of Variations*. Imperial College Press, London.

Gelfand, I. and Fomin, S., 1963. *Calculus of Variations*. Prentice–Hall, Englewood Cliffs. Translated and Edited by R. A. Silverman.

Giles, M. and Pierce, N., 1998. "On the properties of solutions of the adjoint Euler equations". In *Numerical Methods for Fluid Dynamics VI. ICFD*.

Giles, M. and Pierce, N., 2000. "An introduction to the adjoint approach to design". *Flow, Turbulence and Control*, Vol. 65, pp. 393–415.

Goldstein, B., Poole, C. and Safko, J., 2000. *Classical Mechanics*. Addison Wesley, Boston.

Haaser, N.B. and Sullivan, J.A., 1991. *Real Analysis*. Dover, New York.

Haghighi, M., Hawboldt, A., K. and Abdi, M.A., 2015. "Supersonic gas separators: Review of latest developments". *Journal of Natural Gas Science and Engineering*.

Hayashi, M., Ceze, M. and Volpe, E., 2013. "Characteristics–based boundary conditions for the Euler adjoint problem". *International Journal for Numerical Methods in Fluids Vol. 71, No. 10 p. 1297 to 1321*.

Hayashi, M., Ceze, M. and Volpe, E., 2017. "On the Use of the Continuous Adjoint Method to Compute Non–Geometric Sensitivities: Non–Geometric Sensitivities Using The Adjoint Method". *International Journal for Numerical Methods in Fluids*.

Hodge, B.K. and Koenig, K., 2016. *Compressible Fluid Dynamics with personal computer applications*. PearsonIN, Chennai.

Ince, E.L., 1956. *Ordinary Differential Equations*. Longman, Green and Co., London.

Ionescu-Bujor, M., Jin, X. and Cacuci, D.G., 2005. "Deterministic local sensitivity analysis of augmented systems. ii: Applications to the quench–04 experiment using the relap5/mod3.2 code system". *Nuclear Science and Engineering V. 151 p. 67 to 81*.

Jameson, A., 1988. "Aerodynamic design via control theory". In *12th IMACS World Congress on Scientific Computation, MAE Report 1824, Paris, pp. 1 to 40*.

Jameson, A. and Martinelli, L., 2007. "An adjoint method for design optimization of ship hulls". In *9th International Conference on Numerical Ship Hydrodynamics*.

Jameson, A., Pierce, N. and Martinelli, L., 1997. "Optimum aerodynamic design using the Navier-Stokes equations". In *35th Aerospace Sciences Meeting & Exhibit*.

Jameson, A., Pierce, N. and Martinelli, L., 1998. "Optimum aerodynamic design using the Navier-Stokes equations". *Theoretical and Computational Fluid Dynamics*, Vol. 1, pp. 213–237.

Jameson, A., Sriram, A. and Martinelli, L., 2003. "A continuous adjoint method for unstructured grids". In *AIAA Computational Fluid Dynamics Conference*. AIAA 2003–3955.

Jameson, A., 1995. "Optimum aerodynamic design using cfd and control theory". In *AIAA 95-1729-CP*. 95-1729.

Kreyszig, E., 1989. *Introductory Functional Analysis with Applications*. Wiley Classics Library Edition, New York.

Kulfan, B.M. and Bussoletti, J.E., 2006. "Fundamental parametric geometry representations for aircraft component shapes". In *11th AIAA/ISSMO Multidisciplinary Analysis and Optimization Conference*. Portsmouth, VA.

Liberzon, D., 2012. *Calculus of Variations and Optimal Control Theory - A Concise Introduction*. Princeton University Press, Princeton.

Lions, J.L., 1971. *Optimal Control of Systems Governed by Partial Differential Equations*. Number 170= in Die Grundelehren der mathematischen Wissenschaften. Springer–Verlag, Berlin, 1st edition.

Luenberger, D.G., 1969. *Optimization by Vector Space Methods*. John Wiley and Sons, New York.

Lusternick, L. and Sobolev, V., 1961. *Elements of Functional Analysis*. Hindustan Pub. Co., Delhi.

Menter, F.R., 1994. "Two Equation Eddy-Viscosity Turbulence Models for Engineering Applications". *AIAA Journal*, Vol. 32, pp. 1598–1605.

Menter, F.R., 2009. "Review of the shear-stress transport turbulence model experience from an industrial perspective". *International Journal of Computational Fluid Dynamicsl*, Vol. 23, pp. 305–316.

Mohamadi, B. and Pironneau, O., 2000. *Applied shape optimization for fluids*. Oxford Press, Oxford.

Monforte, J.C., 2002. *Geometric, Control and Numerical Aspects of Nonholonomic Systems*. Springer-Verlag, Berlin.

Morse, P.M. and Feshbach, H., 1953. *Methods of Theoretical Physics, Vol. 1*. McGraw-Hill, New York.

Palacios, F. and Economon, T.D.e.a., 2013. "Stanford University Unstructured (SU^2): An open-source integrated computational environment for multi-physics simulation and design, AIAA Paper 2013-0287". In *51st AIAA Aerospace Sciences Meeting and Exhibit. January 7th - 10th, 2013. Grapevine, Texas, USA*. AIAA.

Palacios, F. and Economon, T.D.e.a., 2014. "Stanford University Unstructured (SU2): Open-source analysis and design technology for turbulent flows, AIAA Paper 2014-0243". In *AIAA Science and Technology Forum and Exposition 2014: 52nd Aerospace Sciences Meeting, National Harbor, MD, January 13-17, 2014*. AIAA.

Pironneau, O., 1973. *On Optimal Profiles in Stokes Flow*. Cambridge Press, Cambridge.

Pironneau, O., 1974. *On Optimal Designs in Fluid Dynamics*. Cambridge Press, Cambridge.

Pironneau, O., 1983. *Optimal Shape Design for Elliptic Systems*. Springer Series in Computational Physics. Springer–Verlag, New York.

Smirnov, P.E. and Menter, F.R., 2009. "Sensitization of the SST Turbulence Model to Rotation and Curvature by Applying the Spalart-Shur Correction Term". *ASME Journal of Turbomachinery*, Vol. 131.

Vainberg, M.M., 1964. *Variational Methods for the Study of Nonlinear Operators*. Holden-Day. Translation from the 1956 Russian edition.

Volpe, E.V., 2016. "Introduction to the Adjoint Method, unpublished". Support library.

Zingg, D.W., Nemec, M. and Pulliam, T.H., 2008. "A comparative evaluation of genetic and gradient-based algorithms applied to aerodynamic optimization". *European Journal of Computational Mechanics*, Vol. 17:1–2, pp. 103–126.

7. RESPONSIBILITY NOTICE

The authors are solely responsible for the printed material included in this paper.